Bioconjugate Chemistry

Article

pubs.acs.org/bc

Nanoparticle Encapsulated Lipopeptide Conjugate of Antitubercular Drug Isoniazid: In Vitro Intracellular Activity and in Vivo Efficacy in a Guinea Pig Model of Tuberculosis

Kata Horváti,[†] Bernadett Bacsa,[†] Éva Kiss,[‡] Gergő Gyulai,[‡] Kinga Fodor,[§] Gyula Balka,[∥] Miklós Rusvai,[∥] Eleonóra Szabó,[⊥] Ferenc Hudecz,[†,#] and Szilvia Bősze*,[†]

[†]MTA-ELTE Research Group of Peptide Chemistry, Hungarian Academy of Sciences, [‡]Laboratory of Interfaces and Nanostructures, Institute of Chemistry, and [#]Department of Organic Chemistry, Eötvös L. University, Budapest, 1117 Hungary

[§]Department of State Veterinary Medicine and Agricultural Economics and [∥]Department of Pathology and Forensic Veterinary Medicine, Faculty of Veterinary Science, Szent István University, Budapest, 1078 Hungary

[⊥]Laboratory of Bacteriology, Korányi National Institute for Tuberculosis and Respiratory Medicine, Budapest, 1122 Hungary

ABSTRACT: Considering that *Mycobacterium tuberculosis* (*Mtb*) can survive in host phagocytes for decades and currently applied drugs are largely ineffective in killing intracellular *Mtb*, novel targeted delivery approaches to improve tuberculosis chemotherapy are urgently needed. In order to enhance the efficacy of a clinically used antitubercular agent (isoniazid, INH) a novel lipopeptide carrier was designed based on the sequence of tuftsin, which has been reported as a macrophage-targeting molecule. The conjugate showed relevant in vitro activity on *Mtb* $H_{37}Rv$ culture with low cytotoxicity and hemolytic activity on human cells. The conjugate directly killed intracellular *Mtb* and shows much greater efficacy than free INH. To improve bioavailability, the conjugate was encapsulated into poly(lactide-*co*-glycolide) (PLGA) nanoparticles and tested in vivo in a guinea pig infection model. External clinical signs, detectable mycobacterial colonies in the organs, and the histopathological findings substantiate the potent chemotherapeutic effect of orally administered conjugate-loaded nanoparticles.

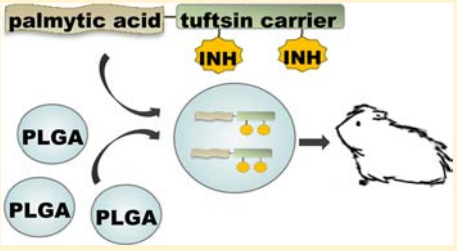

INTRODUCTION

Despite the worldwide availability of antituberculosis drugs, long duration of the treatment, serious adverse effects, poor patient compliance, and the emergence of multidrug-resistant strains indicate that the identification of novel antituberculars, the modification of existing drugs, and the development of new delivery systems to shorten tuberculosis (TB) chemotherapy are urgently needed. Many new drug candidates have been designed from known antibacterial drug classes by synthetic tailoring.[1] Re-engineering of an existing chemical scaffold can improve the antimycobacterial efficacy, safety, and tolerability.[2] For more than 60 years, isoniazid (INH) has been a front-line drug in the battle against *Mycobacterium tuberculosis* (*Mtb*), and it is used as a component of currently applied multidrug chemotherapy of TB. INH is a small hydrophilic molecule that targets mycolic acid biosynthesis and is activated inside the mycobacterial cell by KatG (catalase-peroxidase) enzyme.[3] Pharmacokinetic/pharmacodynamic properties and the potential to cause neurotoxic and hepatotoxic side effects lead the intensive research on the derivatization of INH (reported INH-derivatives have been reviewed along with their biological activity by V. Judge et al.).[4] In a number of studies, high potency of synthetic analogues of INH with increased lipophilicity was found in vitro and in vivo.[5−7]

The incorporation of a lipophilic moiety to the INH scaffold can enhance membrane affinity and penetration into the infected tissues and cells. R. Maccari and her co-workers synthesized and pharmacologically explored numerous different lipophilic analogues of INH with the aim of finding new compounds with activity against TB as well as other AIDS-associated diseases. In the biological assays, general correlation between the lipophilicity and effectiveness of the compounds against intracellular *Mtb* was found.[8−11] Such a property is considered highly predictive for an effective antitubercular agent, since the causative agent of TB can live and multiply inside macrophages.

Exposure to *Mtb* results in a silent, yet persistent infection in the vast majority, during which the *Mtb* bacilli are metabolically slowed down and persist within their host cells for years or even decades. Current TB chemotherapy, while effective in killing actively growing *Mtb*, is largely ineffective in killing persistent or dormant bacilli. The great survival ability of *Mtb* is based on (i) the capability to transform into a stage of dormancy in which the bacillus is shielded by an extremely robust cell wall and renders itself phenotypically resistant to chemotherapy; (ii) the capacity to modulate macrophages and evade phagocytic digestion mechanisms; (iii) initiating the formation of granulomas (the hallmark of TB) which provide a

Received: October 16, 2014
Revised: November 11, 2014
Published: November 13, 2014

   dx.doi.org/10.1021/bc500476x | *Bioconjugate Chem.* 2014, 25, 2260−2268

Scheme 1. Outline of the Synthesis of Conjugate 1[a]

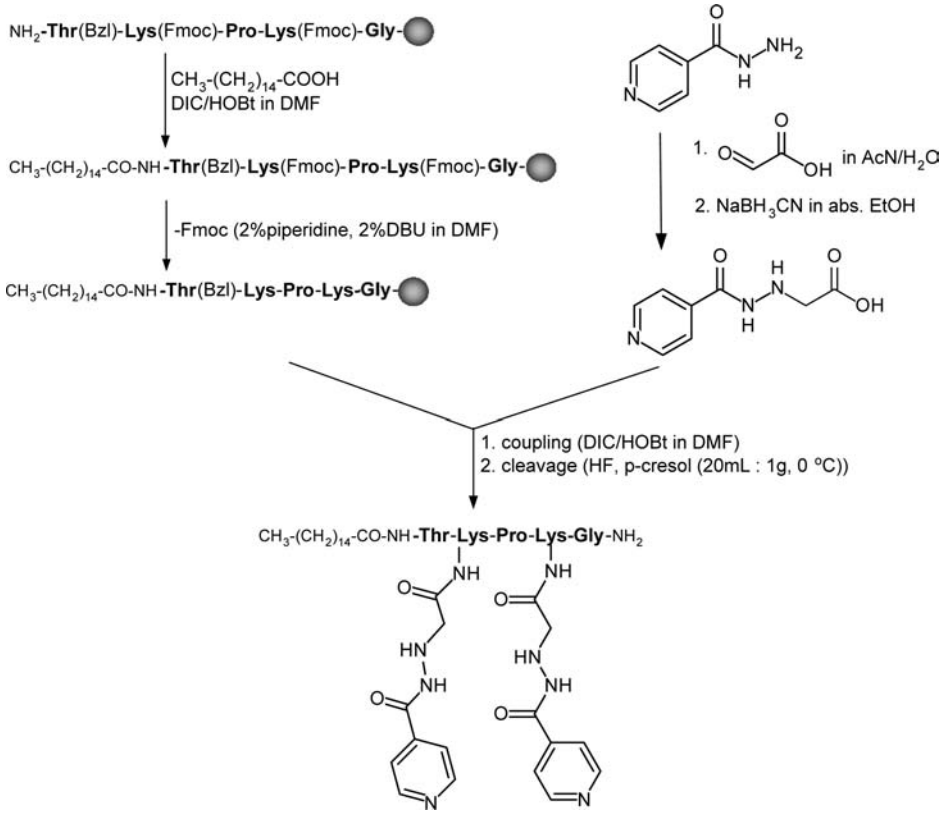

[a]Palmitoylated tuftsin pentapeptide TKPKG was synthesized on solid phase by Boc/Bzl (gray sphere represents the resin). The side chains of the lysine amino acids were protected by Fmoc group which can be selectively removed. INH was first derivatized with glyoxylic acid, then mildly reduced with sodium cyanoborohydride. The resulted hydrazide derivative was conjugated to the free ε-amino groups of the peptide. Conjugate was then cleaved from the resin with liquid HF in the presence of a scavenger.

safety niche for the bacteria.[12] Different in vitro models of mycobacterial persistence have been established over the years, based on oxygen depletion,[13] nutrient starvation,[14] or the use of standing cultures (infection of phagocytic cells or cell lines with *Mtb*).[15] Under certain circumstances, such as anti-TNF-α therapy[16] or immune weakness (HIV/AIDS patients, organ transplants),[17] the dormant *Mtb* bacilli are able to reactivate and cause TB-related clinical signs. One of the most challenging factors in fighting TB is the ability to kill dormant *Mtb*.

For such a purpose we established an advanced drug delivery system for INH: the drug molecule is coupled to a lipopeptide carrier and the conjugate is encapsulated into PLGA nanoparticles. The peptide part of the construct is a tuftsin-related sequence. Tuftsin is a natural phagocytosis stimulating peptide and it has been reported as a macrophage targeting molecule.[18,19] It is estimated that there are 72 000 binding sites available for tuftsin on the surface of phagocytic cells;[20] therefore, tuftsin can be a potent chemical vector for targeted delivery into macrophages through receptor mediated internalization.[21,22] C. M. Gupta and his co-workers have developed tuftsin-bearing liposomes that not only enhance the host's resistance against a variety of infections, but also serve as useful vehicles for the site-specific delivery of drugs in a variety of macrophage-based infections, such as leishmaniasis and TB.[23−26] During the past decade, a new group of sequential oligopeptide carriers has been developed in our laboratory based on the canine tuftsin sequence TKPKG.[27,28] These compounds are nontoxic, nonimmunogenic, and exhibit tuftsin-like biological properties, e.g., receptor-binding and immunstimulatory activity. In the present study, the TKPKG peptide was elongated with palmitic acid to enhance the lipophilicity, membrane affinity, and PLGA encapsulation efficacy.

Encapsulation of drug molecules into nanoparticles is an efficient method for sustained controlled release and is being intensively explored for antitubercular therapy.[29−31] Nanoparticles have the ability to protect the entrapped drug from the external environment, and to delay metabolism and clearance. Over the years, a variety of natural and synthetic polymer-based nanoparticles have been tested as delivery platforms, of which poly(lactide-*co*-glycolide) (PLGA) has been extensively investigated because of its biocompatibility, biodegradability, and wide targeting capability.[32,33] PLGA is approved by the US Food and Drug Administration (FDA) and by the European Medicine Agency (EMA)[34] for clinical use and it can be utilized in various human applications.[35] G. K. Khuller and R. Pandey have published detailed evaluation of INH, rifampin, and pyrazinamide loaded PLGA nanoparticles bearing significant therapeutic potential against experimental TB in guinea pigs and mice.[36−38]

Previously, we reported on a lipopeptide derivative of INH representing enhanced interaction with model lipid membrane[39] and mycolic acid containing monolayer.[40] The conjugate was successfully entrapped in PLGA nanoparticles with highly improved encapsulation efficacy and characterized by high drug content, low polydispersity, and spherical shape within nanometer size.[39]

dx.doi.org/10.1021/bc500476x | *Bioconjugate Chem.* 2014, 25, 2260−2268

In the present work, INH was coupled to a palmitoylated tuftsin peptide derivative to result the pT5i conjugate (**1**). The in vitro selectivity of conjugate **1** was determined by the measurement of the antitubercular efficacy on *Mtb* $H_{37}Rv$ and the hemolytic and cytotoxic effects on human cells. The killing efficacy of **1** on intracellular *Mtb* was also determined. For in vivo evaluation, conjugate **1** was encapsulated into PLGA nanoparticles (**2**) and the chemotherapeutic effect of **2** was measured on *Mtb* infected guinea pigs.

RESULTS

Synthesis and Characterization of pT5i Conjugate (1). The lipopepitde conjugate of INH was prepared by a strategy outlined in Scheme 1. The semiprotected TKPKG pentapeptide [Thr(Bzl)-Lys(Fmoc)-Pro-Lys(Fmoc)-Gly] was synthesized and its *N*-terminal was palmitoylated on solid phase. INH was incorporated into the side chain of two lysine residues using a bifunctional linker entity. After final cleavage, **1** was isolated and carefully characterized by mass spectrometry, analytical HPLC and amino acid analysis. The overall percentage yield of the synthesis—calculated to the capacity of the MBHA resin—was up to 64.8%. The peptide-conjugate content of the lyophilized product was 60.7%. The monoisotopic molecular mass of the conjugate was measured by mass spectrometry (M_{calc} = 1120.6; M_{found} = 1120.7). The purity of the conjugate, which was checked by analytical RP-HPLC, was ≥95%.

Comparison of In Vitro Antitubercular Effect, Cytotoxicity, and Hemolytic Activity. Antitubercular activity of conjugate **1** and the free INH was determined against *Mtb* $H_{37}Rv$ strain. The minimal inhibitory concentration (MIC, the lowest concentration of a compound at which no visible growth of the bacteria occurred) of INH in Sula media was 0.02 mg/L (0.15 μM). The MIC value of conjugate **1** was 0.125 mg/L (0.11 μM). It is interesting to observe that the peptide conjugate of INH proved to be slightly more active than the free drug expressed in molar term (MIC = 0.11 μM for conjugate **1** vs MIC = 0.15 μM for INH).

In order to evaluate the in vitro selectivity we also studied the cytotoxicity and hemolytic activity of the compounds on human PBMC and erythrocytes, respectively. We found that INH and conjugate **1** were not cytotoxic to human PBMC and expressed no hemolytic activity to human erythrocytes even at the highest concentration (for both compounds: IC_{50} > 1000 μM; HC_{50} > 1000 μM).

INH-Lipopeptide Conjugate 1 Kills Intracellular *Mtb*. In order to evaluate drug delivery and intracellular *Mtb* killing efficacy of lipopeptide conjugated INH, we infected human MonoMac6 monocytes with virulent *Mtb* $H_{37}Rv$ bacteria and then the infected cells were treated with the compounds at 100 and 250 mg/L concentrations. The free INH did not exhibit intracellular antitubercular activity even at the higher concentration used (250 mg/L, 1.82 mM). In contrast, conjugate **1** significantly reduced the colony forming units (CFU) of intracellular *Mtb* (Table 1) even at the lower 100 mg/L (0.09 mM) concentration. Considering that the drug content of 100 mg conjugate **1** is 14.8 mg, the affectivity of **1** is more than 16-fold higher than an equivalent amount of free INH.

PLGA Encapsulation of the pT5i Conjugate. In order to improve bioavailability and enable the sustained release, the pT5i conjugate was encapsulated into PLGA nanoparticles as we have previously described.[39] The peptide-conjugate content of the PLGA-pT5i nanoparticles (**2**) was 15.5%, which corresponds to 3.8% free INH content. The encapsulation efficacy of the conjugate **1** was up to 92 ± 7%.

Table 1. Inhibition of Intracellular *Mtb* by INH and by pT5i Conjugate (1)[a]

	CFU[b]	
compound	100 mg/L	250 mg/L
control	+++	+++
INH	+++	+++
pT5i	+	10

[a]Cultured MonoMac6 cells were infected with *Mtb* $H_{37}Rv$ and treated with the compounds at 0.1 and 0.25 mg/mL final concentration. As control, untreated cells were used. The conjugate **1** effectively kill the intracellular *Mtb* bacillus and lower the number of detectable mycobacterial colonies, while free INH was unable to penetrate and kill intracellular bacteria. [b]Colony forming units of *Mtb*, enumerated on Löwenstein-Jensen solid media (+++: confluent colonies; +: 50−100 colonies).

Infection of Guinea Pigs and Signs of Tuberculosis. To analyze the response of guinea pigs to infection with *Mtb* $H_{37}Rv$, external clinical signs and body weight change were monitored weekly in untreated animals. Three infected animals in the control group died at the 13rd, 14th, and 19th week. Signs of the disease, related to TB, such as scuffed fur, body weight loss, and lethargy, were also observed in three other cases. These external clinical signs of TB were further proved by mycobacterial CFU count, detected in spleen, lung, liver, and kidney homogenates as documented in Table 2. Representative sections of tissues were taken from *Mtb* infected animals and histopathology revealed serious involvement by the disease process. The formation of typical tuberculotic lesions, e.g., formation of multiple epitheloid granulomas in the lymph nodes, lungs, liver, and spleen of the infected animals, as a result of type IV, T_H1 mediated hypersensitivity reaction was observed. Multinucleated giant cell formation and/or calcification were also observed in some samples. Ziehl-Neelsen staining demonstrated the acid-fast bacteria in the cytoplasm of the epitheloid cells, or in the multinucleated giant cells (Figure 1).

Comparison of the Chemotherapeutic Effect of Encapsulated INH Conjugate with Free Drug. The effect of PLGA encapsulated INH-conjugate (**2**) as compared with that of the free drug was studied. For this experiment six−six guinea pigs were infected with *Mtb* $H_{37}Rv$ and after 3 weeks of incubation animals were treated orally with **2** or INH twice a week, for a period of 12 weeks. Pharmacokinetics and pharmacodynamics studies suggested that the human-equivalent dose of INH in a guinea pig model of TB chemotherapy is between 30 and 60 mg/kg bw.[41−43] In this study, a 40 mg/kg dose of INH was administered. The dose of **2** was 100 mg/kg bw, which corresponds to approximately 10% (3.8 mg/kg bw) of free INH. As illustrated in Figure 2A, all treated guinea pigs steadily gained weight throughout the whole experiment. No death occurred and no external clinical signs of active TB were observed. The overall response to INH therapy was similar to the treatment with **2** (Figure 2A,B). Oral administration of **2** to *Mtb* infected guinea pigs resulted in undetectable mycobacterial CFU in the lung, liver, and kidney homogenates; however, a number of viable bacteria remained in the spleens of two out of the six animals. In the case of INH treated guinea pigs,

dx.doi.org/10.1021/bc500476x | Bioconjugate Chem. 2014, 25, 2260−2268

Table 2. Mycobacterial Colonies Detected in the Tissues of Treated v Untreated Animals[a]

	INH treated animals						PLGA-pT5i (2) treated animals						control (untreated) animals					
organ	1	2	3	4	5	6	1	2	3	4	5	6	1	2	3	4	5	6
lung	-	-	-	-	-	-	-	-	-	-	-	-	+	++	+	-	-	-
spleen	-	-	-	c.	-	+++	-	++	-	-	-	+++	++	+++	+++	+++	+	-
liver	-	-	-	c.	-	-	-	-	-	-	-	-	+	++	+	++	-	-
kidney	-	-	-	-	-	-	-	-	-	-	-	-	-	++	+	+	-	-

[a]Guinea pigs were infected with *Mtb* H_{37}Rv and treated with PLGA encapsulated pT5i conjugate (**2**) or free INH. The tuberculotic involvement of the tissues was proven by colony forming unit (CFU) determination from the homogenates, enumerated on Löwenstein-Jensen solid media. In the case of treatment with **2** no mycobacterial colonies were observed except in the tissue homogenates of spleen of two animals, which was comparable to free INH treatment. In contrast, in most of the tissues of untreated control animals, colonies of *Mtb* were detected. +++: confluent colonies; ++: innumerable colonies, but not confluent; +: 50−100 colonies; -: no colonies were observed; c.: contamination.

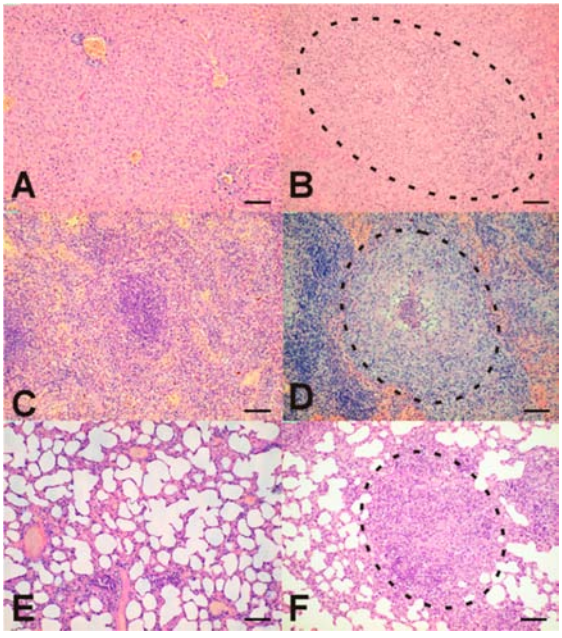

Figure 1. Histological picture of different normal (left side) and tuberculosis affected (right side) organs. Six-week-old, inbred female guinea pigs were infected by intramuscular injection with virulent *Mtb* H_{37}Rv culture. After necropsy procedure, organs were removed and fixed in formalin for histopathological analysis. Tissue specimens were embedded, sectioned, and stained with hematoxylin and eosin (HE). For in situ visualization of the acid-fast bacilli the Ziehl−Neelsen (ZN) staining method was applied. (A,B) − liver; (C,D) − spleen; (E,F) − lung; dashed circles indicate the tuberculotic epitheloid granulomas in the pictures. The histopathological findings clearly demonstrate the development of active tuberculosis in the case of untreated infected animals. HE. 100× Bar, 100 μm.

comparable results were found: one of the six animals presented countable CFU in the spleen (Table 2).

In Vivo Toxicology. In order to analyze the potential adverse effects of the treatment with **2**, three guinea pigs were administered the dose of 100 mg/kg bw orally twice a week. As control, three guinea pigs were treated with INH (40 mg/kg bw) with the same frequency. During the experiment animals maintained a constant weight gain, as shown in Figure 3, and no symptoms, related to compound toxicity, were observed. Namely, there were no significant differences in the change in body weight between **2** and INH treated groups of animals. After 7 weeks of administration of **2** and INH, animals were euthanized and the diagnostic autopsy involving lung, spleen, liver, kidney, and heart proved that no significant malformations on the tissues occurred. It should also be noted that no hepatotoxicity was observed in any of animals receiving treatment with **2** or INH.

DISCUSSION

The current standard regimen for TB therapy requires 6 to 9 months of a daily administered combination of various drugs in which patient noncompliance often results in treatment failure.[44] Shorter treatment, reduced dose, and reduced dosing frequency could be achieved not only with novel drug entities, but also with appropriate drug delivery systems aimed at sustained release of antituberculars and/or targeted transport to intracellular bacteria. Drug conjugation to a macrophage targeting molecule, such as tuftsin,[18,19] has the potential to improve intracellular disease therapy.

In this study INH, a front-line antitubercular drug, was covalently conjugated to a palmitoylated tuftsin derivative with a sequence of TKPKG. From the in vitro evaluation of the antimycobacterial activity of conjugate **1**, we can conclude that INH maintained its antimicrobial efficacy indicating that the applied hydrazide modification of the INH is permitted. Therefore, this synthetic route can be used for the tailoring of INH molecule. Furthermore, the use of glyoxylic acid as a bifunctional linker represents a convenient method to selectively conjugate INH to peptides or other carrier molecules bearing available amino groups.

The incorporation of a fatty acid moiety into the *N*-terminal of the peptide part of the conjugate enhanced the hydrophobicity which was characterized by the increase of the log *P* value from −1.14 (INH) to −0.2 (conjugate **1**).[39] Furthermore, high membrane affinity and significant penetration ability was observed for the pT5i conjugate in a Langmuir monolayer model containing mycolic acid.[40] It is also believed that increased lipophilicity of INH can play an important role in its antimycobacterial activity against susceptible and resistant *Mtb* strains.[45]

The antitubercular effect of the conjugate was assayed on the well-characterized virulent *Mtb* laboratory strain H_{37}Rv. We have also studied the in vitro cytotoxicity of the conjugate to human PBMC and to human erythrocytes. From these results the selectivity index was calculated: SI [the ratio of cell cytotoxicity over minimal inhibitory concentration against *Mtb* (IC_{50}/MIC)] > 8000 for the conjugate **1** and SI > 8000 for INH.

It was also proven that conjugate **1** is effective against intracellular *Mtb* and significantly reduces the viability of persisting bacteria. It is interesting to note that the treatment of *Mtb* infected monocytes with conjugate **1** was highly successful, resulting only a few colonies at 100 mg/L, while the treatment with INH resulted in confluent colonies which represent the

dx.doi.org/10.1021/bc500476x | *Bioconjugate Chem.* 2014, 25, 2260−2268

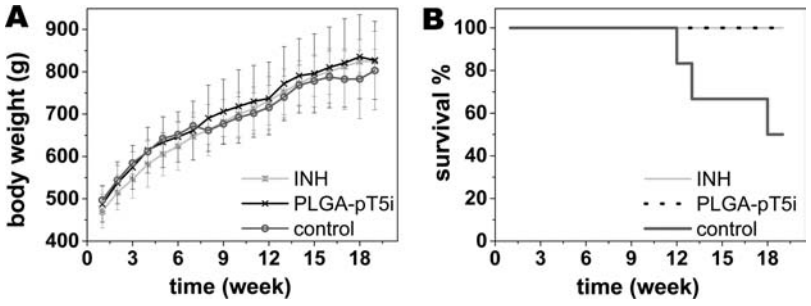

Figure 2. Chemotherapeutic effect of PLGA-pT5i (**2**) compared to INH on *Mtb* infected guinea pigs. Weight gain (A) and survival rate (B) of treated vs untreated animals. Guinea pigs were infected with *Mtb* $H_{37}Rv$ intramuscularly; then after 3 weeks of incubation, 6−6 animals were treated with **2** (100 mg/kg bw) or with INH (40 mg/kg bw) orally twice a week. Control animals were administered 1 mL sterile water orally with the same frequency. None of the treated animals died during the 133-day long experiment, while the survival rate of untreated animals was 50% (3/6). Weight gain of **2** treated animals was similar to that of INH treated animals. In both groups guinea pigs steadily gained weight and no external clinical signs of tuberculosis were observed.

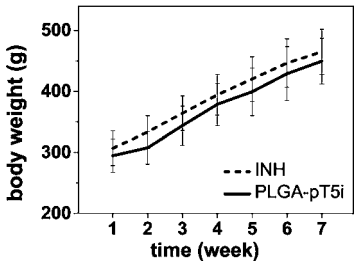

Figure 3. Weight gain of INH and PLGA-pT5i (**2**) treated guinea pigs. Three guinea pigs were administered orally 100 mg/kg bw **2** twice a week for 7 weeks (solid line). As control experiment, 3 guinea pigs were treated with 40 mg/kg bw INH for 7 weeks with the same frequency (dashed line). In both treatment groups, animals maintained constant weight gain.

inefficacy of the free drug against intracellular bacteria. This could be explained by the fact that the lipopeptide carrier used was efficient to deliver INH to its intracellular target. Subsequently, we performed in vivo experiments to evaluate the chemotherapeutic activity and toxic side effects of conjugate **1**.

The fast degradation of a peptide-based conjugate after oral administration can be avoided by encapsulation into nanoparticles and the biodistribution of an active compound can be essentially modified with this method. PLGA encapsulation is a cost-effective, practical formulation of drugs and the release rate can be controlled by the size and composition of the particles.[46] Both PLGA and Pluronic block copolymers are approved by the US and European medicine agencies in various drug delivery systems.[34] The encapsulation efficacy of conjugate **1** was above 90%, which represents a remarkable increase compared to free INH. As reported previously,[39] the drug content of free INH loaded PLGA nanoparticles was 0.5% and the encapsulation efficacy of INH was only 10%. The higher loading capacity is a further advantage of the lipopeptide conjugation used and increased hydrophobicity. The pT5i loaded PLGA nanoparticles (**2**) were spherical and the size was in the nanometer range with low polydispersity. Furthermore, freeze−dried samples were easily redispersed and the size and polydispersity—which was checked occasionally by DSL—was the same as before lyophilization.

For the determination of in vivo chemotherapeutic effect, the guinea pig infectious model was employed. Guinea pigs are highly susceptible to infection with *Mtb* and develop a disease that is observed in humans, including the formation of granuloma, pulmonary lesions, and caseation necrosis.[47−49] Guinea pigs were infected with a virulent *Mtb* $H_{37}Rv$ strain. The external clinical signs, detectable mycobacterial CFU in the organs (Table 2), and microscopic findings (Figure 1) clearly demonstrate the development of TB in the case of control animals. The in vivo antitubercular effect of **2** was compared to free INH. Forty mg/kg bw dose of INH was administered orally twice a week to the infected guinea pigs. The dose of nanocapsules **2** was 100 mg/kg bw which corresponds to approximately 10% (3.8 mg/kg bw) of free INH. After necropsy procedure, the histopathological examination of the tissues revealed that treatment with **2** has resulted in considerably decreased inflammation and minimal granulomatous involvement compared to untreated control. A similar result was found in the overall response to INH therapy, while the INH content was only 1/10 that in the conjugate loaded nanocapsules. Furthermore, no symptoms related to compound toxicity were observed during the experiment.

As a summary of this study we can conclude that a new type of lipopeptide based conjugation and nanoparticle encapsulation was applied for INH with relevant chemotherapeutic efficacy against experimental TB. The conjugate **1** led to killing of intracellular *Mtb* in infected monocytes, providing proof of principle for this targeting technology. PLGA entrapped lipotuftsin conjugation of antituberculars represents a promising delivery system for developing improved therapy for TB, and further pharmacokinetic profile of the nanocapsule **2** is worth investigating.

EXPERIMENTAL PROCEDURES

Materials. Amino acid derivatives and palmitic acid were obtained from Reanal (Budapest, Hungary), except Boc-Lys(Fmoc)-OH which was from NovaBiochem (Läufelfingen, Schwitzerland). MBHA resin (capacity = 1.2 mmol/g, 100−200 mesh), 1-hydroxybenzotriazole (HOBt), and 1,8-diazabicyclo[5.4.0]undec-7-ene (DBU) were purchased from IRIS Biotech (Marktredwitz, Germany). Isoniazid, glyoxylic acid monohydrate, *N,N*-diisopropylethylamine (DIEA), and *N,N′*-diisopropylcarbodiimide (DIC) were purchased from Fluka (Buchs, Switzerland). Acetonitrile, trifluoroacetic acid (TFA), *N*-methylpyrrolidone (NMP), dimethyl sulfoxide (DMSO), $NaBH_3CN$, carbol-fuchsin, and hematoxylin were from Merck (Darmstadt, Germany). *N,N*-Dimethylformamide

dx.doi.org/10.1021/bc500476x | *Bioconjugate Chem.* 2014, 25, 2260−2268

(DMF), dichloromethane (DCM), and eosin were also from Reanal (Budapest, Hungary).

For the nanoparticle preparation poly(DL-lactide-*co*-glycolide), PLGA with 50% of lactic and 50% of glycolic content (Mw: 50 000−75 000), obtained from Sigma-Aldrich (St. Louis, MO, USA), and poly(ethylene oxide)/poly(propylene oxide)/poly(ethylene oxide), PEO−PPO−PEO triblock copolymer, Pluronic 12700 provided by BASF Hungaria Kft. (Budapest, Hungary), were applied as received.

For the in vitro assays RPMI-1640 medium (with or without phenol red), fetal calf serum (FCS), nonessential amino acids, 3-(4,5-dimethyltiazol-2-yl)-2,5-diphenyl tetrazolium bromide (MTT), Löwenstein-Jensen and Sula medium base were obtained from Sigma-Aldrich (St. Louis, MO, USA).

Synthesis of pT5i Conjugate (1). Protected tuftsin derivate (TKPKG, T5) was produced manually by solid-phase synthesis on MBHA resin using Boc/Bzl strategy. The following amino acid derivatives were used: Boc-Gly-OH, Boc-Lys(Fmoc)-OH, Boc-Pro-OH, and Boc-Thr(Bzl)-OH. Protocol of the synthesis was as follows: (i) Boc deprotection with TFA/DCM (1:3 v/v) mixture (2 + 20 min); (ii) neutralization with DIEA/DCM (1:10 v/v) (5 × 1 min); (iii) coupling 3 equiv of Boc-amino acid derivative − DIC − HOBt dissolved in NMP (60 min); (iv) ninhydrin or isatin assay. After Boc deprotection of the *N*-terminal amino acid, palmitic acid was coupled (3 equiv) to the *N*-terminus of the peptide in the presence of DIC and HOBt (3−3 equiv) reagents (60 min). Then, the N^{ε}-Fmoc protecting group of the side chain of Lys residues was selectively removed with piperidine/DBU/DMF (2:2:96 v/v) solution (2 + 2 + 5 + 20 min).

In parallel, an INH derivative was prepared for conjugation: INH was reacted with glyoxylic acid monohydrate (1 to 1 equiv) in acetonitrile/water (1:4 v/v)). After 1 h stirring, the precipitate was filtered, washed with water and acetonitrile, and dried over P_2O_5 under vacuum. After the hydrazine bond formation the compound was reduced with $NaBH_3CN$ in abs ethanol as described previously.[50]

The product, isonicotinoylhydrazinoacetic acid (6 equiv), was added to the peptidyl-resin described above in the presence of 6 equiv of DIC and HOBt. PT5i peptide conjugate was cleaved from the resin with liquid HF in the presence of *p*-cresol (20 mL: 1 g) (0 °C, 1.5 h), precipitated with cold abs diethyl ether, dissolved in water, and freeze−dried.

Analytical Characterization of pT5i Conjugate (1). The final product was characterized by mass spectrometry, analytical HPLC, and amino acid analysis. The conjugate **1** possesses a purity of ≥95%.

Mass spectrometric analyses were performed on a Bruker Esquire 3000+ ion trap mass spectrometer (Bruker, Bremen, Germany) equipped with electrospray ionization (ESI) source. Samples were dissolved in a mixture of acetonitrile/water = 1/1 (v/v) containing 0.1% acetic acid and introduced by a syringe pump with a flow rate of 10 μL/min.

The homogeneity of the compounds was checked by analytical HPLC using a laboratory-assembled Knauer HPLC system (Bad Homburg, Germany) with an Eurospher-100 C-4 column (250 × 4 mm, 5 μm particle size, 300 Å pore size) (Knauer). The gradient elution system consisted of 0.1% TFA in water (eluent A) and 0.1% TFA in acetonitrile/water = 80/20 (v/v) (eluent B). The eluent B content was 25% for 5 min, then varied from 25% to 100% in 35 min with 1 mL/min flow rate at room temperature. Twenty microliters of sample was injected and peaks were detected at λ = 214 nm.

Amino acid analysis was performed on a Sykam Amino Acid S433H analyzer (Eresing, Germany) equipped with an ion exchange separation column and postcolumn derivatization. Prior to analysis, samples were hydrolyzed with 6 M HCl in sealed and evacuated tubes at 110 °C for 24 h. For postcolumn derivatization the ninhydrin-method was used.

Preparation and Characterization of Conjugate 1 Loaded PLGA Nanoparticle (2). PLGA nanoparticles were prepared by the nanoprecipitation (solvent exchange) method similar to that employed previously.[39] Briefly, 85 mg PLGA and 60 mg conjugate **1** were dissolved in 8.5 mL acetone and added dropwise to 34 mL of 2 g/L aqueous solution of Pluronic 12700 with magnetic stirring at room temperature. Nanoparticles formed and the stirring was continued until complete evaporation of the organic solvent. The resulting particle suspension was centrifuged at 6000 rpm for 10 min to remove the possible polymer aggregates. The amount of that sediment was always less than 5% of the whole solid content. The nanoparticle suspension was purified by dialysis against water and freeze−dried.

Drug content of the lyophilized powder of **2** was determined by amino acid analysis as described above.

The size of the nanoparticles was determined by dynamic light scattering (DLS) and morphology and the size distribution was studied by scanning electron microscopy (SEM) (detailed in ref 39).

In Vitro Assays. *Determination of Antitubercular Activity.* In vitro antitubercular activity of the compounds was determined against *Mycobacterium tuberculosis* $H_{37}Rv$ (ATCC 27294) by serial dilution method in Sula semisynthetic medium (prepared in-house).[51−53] Compounds were added to 5 mL of Sula medium as 10 μL aqueous solutions in duplicates (range of final concentrations was between 0.005 and 5 mg/L). Each tube was inoculated with 0.5 McFarland bacteria and the minimal inhibitory concentration (MIC) was determined after incubation at 37 °C for 28 days. MIC was the lowest concentration of a compound at which no visible growth of the bacteria occurred. The activities of the tested compounds were confirmed using colony forming unit (CFU) determination by subculturing from the Sula medium onto drug-free Löwensten-Jensen solid medium (37 °C, 28 days). Experiments were repeated at least two times.

Analysis of Hemolytic Activity. In vitro hemolytic activity of the compounds was determined as described previously.[54] Briefly, peripheral blood from healthy volunteers was collected in vacuum tubes containing heparin (Li-heparin LH, VenoSafe) as anticoagulant. Tubes were centrifuged (1000 rpm, 5 min), the pellet was washed 3 times with RPMI-1640 (culturing media without phenol red), and RPMI-1640 was added enough to yield 8 v/v% erythrocyte suspension. Compounds were dissolved in the same buffer and a 3-fold serial dilution series were prepared. Red blood cell suspension (100 μL/well) was placed into a 96-well cell culture plate and mixed with 100 μL compound solution to result 4 v/v% final erythrocyte concentration. The plates were incubated for 4 h at 37 °C. After centrifugation (1500 rpm, 5 min), 100 μL of the supernatant was transferred to a flat-bottom microtiter plate, and absorbance was measured at 450 nm. The percentage hemolysis was compared to 1 mg/mL SDS treated erythrocytes and the HC_{50} values, which represent the concentrations of compound at which 50% hemolysis was observed, were determined. Each assay was performed in 4 replicates.

Cell Culturing and Cytotoxicity Assay. Peripheral blood mononuclear cells (PBMC) were prepared from peripheral blood of healthy volunteers using Ficoll-Hypaque density gradient centrifugation method. PBMC were cultured in complete medium prepared from RPMI-1640 supplemented with 10% FCS, 2 mM L-glutamine, and 160 μg/mL gentamycin at 37 °C in 5% CO_2 atmosphere. Twenty-four hours prior to treatment, PBMC cells were plated into a 96-well round-bottom plate (250 000 cell/100 μL complete medium).

Prior to treatment, cells were washed with serum-free RPMI-1640 medium. Compounds to be tested were dissolved in serum-free medium and added to the cells to give 0.5−1000 μM final concentration. Cells were incubated with the compounds for 4 h, then cell viability was tested using the MTT (3-(4,5-dimethyltiazol-2-yl)-2,5-diphenyl tetrazolium bromide) test.[55−57] Briefly, 45 μL MTT solutions were added to each well (2 mg/mL, solved in serum-free medium). Following 4 h of incubation, plates were centrifuged at 2000 rpm for 5 min, and the supernatant was carefully aspirated with a G30 needle. The precipitated purple crystals were dissolved in 100 μL DMSO, and after 10 min agitation, the absorbance was determined at λ = 540 and 620 nm using ELISA plate reader (iEMS Reader, Labsystems). The measured cytotoxicity in percentage as a function of compound concentration was represented graphically using Microcal Origin 8.6 software. IC_{50} value is the mean of 4 parallel experiments and represents the concentration of the compound which is required for 50% inhibition.

Determination of Intracellular Antitubercular Activity. Infection of MonoMac6 cells with *Mtb* H_{37}Rv and the efficacy against intracellular *Mtb* bacteria were determined using a modified method based on previously published works.[15,58,60] Briefly, MonoMac6 human monocytic cell line (DSMZ no.: ACC 124, Braunschweig, Germany)[59] was maintained in RPMI-1640 medium containing 10% FCS, 2 mM L-glutamine, and 160 μg/mL gentamycin at 37 °C in 5% CO_2 atmosphere. Prior to experiment, cells were cultured in a 24-well plate for 24 h (2×10^5 cells/1 mL medium/well). Adherent cells were infected with *Mtb* H_{37}Rv at a multiplicity of infection (MOI) of 10 for 4 h. Nonphagocytized extracellular bacteria were removed and the culture was washed three times with serum free RPMI. The infected monolayer was incubated for 1 day before antitubercular treatment. Infected cells were then treated with the compounds at 100 and 250 mg/L final concentrations. After 3 days the treatment was repeated with fresh solution of the compounds for an additional 3 days. Untreated cells were considered as a negative control. As control compound, INH was used at 100 and 250 mg/L final concentration. After washing steps—in order to remove the antituberculars—infected cells were lysed with 2.5% sodium dodecyl sulfate solution. The CFU of *Mtb* was enumerated on Löwenstein-Jensen solid media after 4 weeks of incubation. Experiments were repeated at least twice.

In Vivo Evaluation. *Animals and Ethics Statement.* Inbred female guinea pigs aged 6 weeks at weight 400−500 g were housed four per cage and allowed free access to water and to standard pellet diet. All animal experiments were approved by the Hungarian Scientific Ethical Committee on Animal Experimentation (No: 22.1/3720/003/2009), and all efforts were made to minimize suffering.

Experimental Infection and Chemotherapy. After 4 weeks of incubation, guinea pigs were infected by intramuscular injection with 1.5×10^8 viable bacilli of *Mtb* H_{37}Rv in a volume of 0.1 mL of Sula medium.

Chemotherapy was started 3 weeks after infection. Guinea pigs were divided into three different groups of 6 animals: INH treated animals (group 1); **2** treated animals (group 2); untreated controls (group 3). Forty mg/kg bw INH and 100 mg/kg bw of **2** were suspended in 1 mL sterile water and administered orally twice a week. Control animals were administered 1 mL of sterile water with the same frequency.

Necropsy Procedure, CFU Determination, and Histopathology. After 12 weeks of chemotherapy, animals were euthanized by ketamine (40 mg/kg bw) and dexmedetomidine (Dexdomitor, 0.5 mg/kg bw). To count the number of bacteria in the organs, a portion of lung, spleen, liver, and kidney were resected and homogenized in Sula media. 100 μL aliquots of 1:1000 dilution of the homogenates were plated onto Löwenstein-Jensen solid media, and after 8 weeks of incubation at 37 °C in 5% CO_2 atmosphere, CFU was enumerated.

For histopathological analysis, lung, spleen, liver, kidney, inguinal lymph nodes, and heart muscle of each animal were removed and fixed in 8% neutral buffered formalin for 24 h at room temperature. Tissue specimens were dehydrated in a series of ethanol and xylene baths and embedded in paraffin wax. Sections (3−4 μm) were cut, mounted on Super Frost Ultra Plus slides (Thermo Scientific, Menzel-Gläser, Braunschweig, Germany), deparaffinized in xylene and graded ethanol, and stained with hematoxylin and eosin (HE). For in situ visualization of the acid-fast bacilli Ziehl−Neelsen (ZN) staining method was applied on similarly pretreated sections. This method is based on the highly resistant bacterial wall of Mycobacteria that retain the original red dye (Carbol-Fuchsin) after destaining with 3% hydrochloric acid in alcohol. Acid fast Mycobacteria appear as red rods in these sections, whereas all other bacteria and tissue components are blue according to the final hematoxylin counterstaining.

In Vivo Toxicology. Six-week-old inbred female guinea pigs (250−350 g) were housed and fed as described above. Animals were administered 100 mg/kg bw of **2** orally twice a week (group 1), or 40 mg/kg bw of INH (group 2) (n = 3 for each treatment group). To monitor the side effects of the chemotherapy, changes in body weight were determined weekly. After 7 weeks of administration, animals were euthanized and diagnostic autopsy was evaluated.

AUTHOR INFORMATION

Corresponding Author

*Tel: +36-1-372-2500 ext. 1736, fax: +36-1-372-2620, e-mail: bosze@elte.hu.

Notes

The authors declare no competing financial interest.

ACKNOWLEDGMENTS

The authors thank Dr. Hedvig Medzihradszky-Schweiger for the amino acid analyses and to Mr. Sándor Dávid for performing the antimycobacterial tests. This work was supported by the Hungarian Research Fund (T68358, T68285, 104928, 104275); by the Social Renewal Operational Programme (TÁMOP-4.2.2.B-10/1, Development of a complex educational assistance/support system for talented students and prospective researchers at the Szent István University" project), and by the National Research and Development Programme (NKFP_07_1-TB_INTER-HU).

REFERENCES

(1) Fischbach, M. A., and Walsh, C. T. (2009) Antibiotics for emerging pathogens. *Science 325*, 1089−1093.

(2) Koul, A., Arnoult, E., Lounis, N., Guillemont, J., and Andries, K. (2011) The challenge of new drug discovery for tuberculosis. *Nature 469*, 483−490.

(3) Zhang, Y., Heym, B., Allen, B., Young, D., and Cole, S. (1992) The catalase-peroxidase gene and isoniazid resistance of mycobacterium tuberculosis. *Nature 358*, 591−593.

(4) Judge, V., Narasimhan, B., and Ahuja, M. (2012) Isoniazid: The magic molecule. *Med. Chem. Res. 21*, 3940−3957.

(5) Rastogi, N., and Goh, K. S. (1990) Action of 1-isonicotinyl-2-palmitoyl hydrazine against the mycobacterium avium complex and enhancement of its activity by m-fluorophenylalanine. *Antimicrob. Agents Chemother. 34*, 2061−2064.

(6) Hearn, M. J., Cynamon, M. H., Chen, M. F., Coppins, R., Davis, J., Kang, H. J. O., Noble, A., Tu-Sekine, B., Terrot, M. S., Trombino, D., Thai, M., Webster, E. R., and Wilson, R. (2009) Preparation and antitubercular activities in vitro and in vivo of novel schiff bases of isoniazid. *Eur. J. Med. Chem. 44*, 4169−4178.

(7) Sriram, D., Yogeeswari, P., and Priya, D. Y. (2009) Antimycobacterial activity of novel n-(substituted)-2-isonicotinoylhydrazinocarbothioamide endowed with high activity towards isoniazid resistant tuberculosis. *Biomed. Pharmacother. 63*, 36−39.

(8) Maccari, R., Ottana, R., Bottari, B., Rotondo, E., and Vigorita, M. G. (2004) In vitro advanced antimycobacterial screening of cobalt(ii) and copper(ii) complexes of fluorinated isonicotinoylhydrazones. *Bioorg. Med. Chem. Lett. 14*, 5731−5733.

(9) Maccari, R., Ottana, R., Monforte, F., and Vigorita, M. G. (2002) In vitro antimycobacterial activities of 2′-monosubstituted isonicotinohydrazides and their cyanoborane adducts. *Antimicrob. Agents Chemother. 46*, 294−299.

(10) Maccari, R., Ottana, R., and Vigorita, M. G. (2005) In vitro advanced antimycobacterial screening of isoniazid-related hydrazones, hydrazides and cyanoboranes: Part 14. *Bioorg. Med. Chem. Lett. 15*, 2509−2513.

(11) Vigorita, M. G., Ottana, R., Maccari, R., Monforte, F., Bisignano, G., and Pizzimenti, F. C. (1998) Synthesis and in vitro antimicrobial and antitumoral screening of novel lipophilic isoniazid analogues. Vi. *Boll. Chim. Farm. 137*, 267−276.

(12) Gengenbacher, M., and Kaufmann, S. H. (2012) Mycobacterium tuberculosis: Success through dormancy. *FEMS Microbiol. Rev. 36*, 514−532.

(13) Wayne, L. G. (2001) In vitro model of hypoxically induced nonreplicating persistence of mycobacterium tuberculosis. *Methods Mol. Med. 54*, 247−269.

(14) Betts, J. C., Lukey, P. T., Robb, L. C., McAdam, R. A., and Duncan, K. (2002) Evaluation of a nutrient starvation model of mycobacterium tuberculosis persistence by gene and protein expression profiling. *Mol. Microbiol. 43*, 717−731.

(15) Wright, E. L., Quenelle, D. C., Suling, W. J., and Barrow, W. W. (1996) Use of mono mac 6 human monocytic cell line and j774 murine macrophage cell line in parallel antimycobacterial drug studies. *Antimicrob. Agents Chemother. 40*, 2206−2208.

(16) Gardam, M. A., Keystone, E. C., Menzies, R., Manners, S., Skamene, E., Long, R., and Vinh, D. C. (2003) Anti-tumour necrosis factor agents and tuberculosis risk: Mechanisms of action and clinical management. *Lancet Infect. Dis. 3*, 148−155.

(17) Maartens, G., and Wilkinson, R. J. (2007) Tuberculosis. *Lancet 370*, 2030−2043.

(18) Siemion, I. Z., and Kluczyk, A. (1999) Tuftsin: On the 30-year anniversary of Victor Najjar's discovery. *Peptides 20*, 645−674.

(19) Tripathi, S. K., Goyal, R., Kashyap, M. P., Pant, A. B., Haq, W., Kumar, P., and Gupta, K. C. (2012) Depolymerized chitosans functionalized with bpei as carriers of nucleic acids and tuftsin-tethered conjugate for macrophage targeting. *Biomaterials 33*, 4204−4219.

(20) Barshavit, Z., Goldman, R., Stabinsky, Y., and Fridkin, M. (1979) Tuftsin-macrophage interaction - specific binding and augmentation of phagocytosis. *J. Cell. Physiol. 100*, 55−62.

(21) Amoscato, A. A., Davies, P. J., Babcock, G. F., and Nishioka, K. (1983) Receptor-mediated internalization of tuftsin. *Ann. N.Y. Acad. Sci. 419*, 114−134.

(22) Gottlieb, P., Stabinsky, Y., Hiller, Y., Beretz, A., Hazum, E., Tzehoval, E., Feldman, M., Segal, S., Zakuth, V., Spirer, Z., and Fridkin, M. (1983) Tuftsin receptors. *Ann. N.Y. Acad. Sci. 419*, 93−106.

(23) Agarwal, A., Kandpal, H., Gupta, H. P., Singh, N. B., and Gupta, C. M. (1994) Tuftsin-bearing liposomes as rifampin vehicles in treatment of tuberculosis in mice. *Antimicrob. Agents Chemother. 38*, 588−593.

(24) Agrawal, A. K., Agrawal, A., Pal, A., Guru, P. Y., and Gupta, C. M. (2002) Superior chemotherapeutic efficacy of amphotericin b in tuftsin-bearing liposomes against leishmania donovani infection in hamsters. *J. Drug Targeting 10*, 41−45.

(25) Gupta, C. M., and Haq, W. (2005) Tuftsin-bearing liposomes as antibiotic carriers in treatment of macrophage infections. *Methods Enzymol. 391*, 291−304.

(26) Guru, P. Y., Agrawal, A. K., Singha, U. K., Singhal, A., and Gupta, C. M. (1989) Drug targeting in leishmania-donovani infections using tuftsin-bearing liposomes as drug vehicles. *FEBS Lett. 245*, 204−208.

(27) Mező, G., Kalászi, A., Reményi, J., Majer, Z., Hilbert, A., Láng, O., Kőhidai, L., Barna, K., Gaal, D., and Hudecz, F. (2004) Synthesis, conformation, and immunoreactivity of new carrier molecules based on repeated tuftsin-like sequence. *Biopolymers 73*, 645−656.

(28) Bai, K. B., Láng, O., Orbán, E., Szabó, R., Kőhidai, L., Hudecz, F., and Mező, G. (2008) Design, synthesis, and in vitro activity of novel drug delivery systems containing tuftsin derivatives and methotrexate. *Bioconjugate Chem. 19*, 2260−2269.

(29) Pandey, R., and Ahmad, Z. (2011) Nanomedicine and experimental tuberculosis: Facts, flaws, and future. *Nanomedicine 7*, 259−272.

(30) Gelperina, S., Kisich, K., Iseman, M. D., and Heifets, L. (2005) The potential advantages of nanoparticle drug delivery systems in chemotherapy of tuberculosis. *Am. J. Resp. Crit. Care Med. 172*, 1487−1490.

(31) Sosnik, A., Carcaboso, A. M., Glisoni, R. J., Moretton, M. A., and Chiappetta, D. A. (2010) New old challenges in tuberculosis: Potentially effective nanotechnologies in drug delivery. *Adv. Drug Delivery Rev. 62*, 547−559.

(32) Bala, I., Hariharan, S., and Kumar, M. N. (2004) Plga nanoparticles in drug delivery: The state of the art. *Crit. Rev. Ther. Drug Carrier Syst. 21*, 387−422.

(33) Shive, M. S., and Anderson, J. M. (1997) Biodegradation and biocompatibility of PLA and PLGA microspheres. *Adv. Drug Delivery Rev. 28*, 5−24.

(34) Danhier, F., Ansorena, E., Silva, J. M., Coco, R., Le Breton, A., and Preat, V. (2012) PLGA-based nanoparticles: An overview of biomedical applications. *J. Controlled Release 161*, 505−522.

(35) Ul-Ain, Q., Sharma, S., and Khuller, G. K. (2003) Chemotherapeutic potential of orally administered poly(lactide-co-glycolide) microparticles containing isoniazid, rifampin, and pyrazinamide against experimental tuberculosis. *Antimicrob. Agents Chemother. 47*, 3005−3007.

(36) Pandey, R., Sharma, A., Zahoor, A., Sharma, S., Khuller, G. K., and Prasad, B. (2003) Poly (dl-lactide-co-glycolide) nanoparticle-based inhalable sustained drug delivery system for experimental tuberculosis. *J. Antimicrob. Chemother. 52*, 981−986.

(37) Pandey, R., Zahoor, A., Sharma, S., and Khuller, G. K. (2003) Nanoparticle encapsulated antitubercular drugs as a potential oral drug delivery system against murine tuberculosis. *Tuberculosis (Edinburgh) 83*, 373−378.

(38) Sharma, A., Pandey, R., Sharma, S., and Khuller, G. K. (2004) Chemotherapeutic efficacy of poly (dl-lactide-co-glycolide) nanoparticle encapsulated antitubercular drugs at sub-therapeutic dose

against experimental tuberculosis. *Int. J. Antimicrob. Agents 24*, 599−604.
(39) Kiss, É., Schnöller, D., Pribranska, K., Hill, K., Pénzes, C. B., Horváti, K., and Bősze, S. (2011) Nanoencapsulation of antitubercular drug isoniazid and its lipopeptide conjugate. *J. Dispersion Sci. Technol. 32*, 1728−1734.
(40) Pénzes, C. B., Schnöller, D., Horváti, K., Bősze, S., Mező, G., and Kiss, É. (2012) Membrane affinity of antituberculotic drug conjugate using lipid monolayer containing mycolic acid. *Colloids Surf., A 413*, 142−148.
(41) Ahmad, Z., Klinkenberg, L. G., Pinn, M. L., Fraig, M. M., Peloquin, C. A., Bishai, W. R., Nuermberger, E. L., Grosset, J. H., and Karakousis, P. C. (2009) Biphasic kill curve of isoniazid reveals the presence of drug-tolerant, not drug-resistant, mycobacterium tuberculosis in the guinea pig. *J. Infect. Dis. 200*, 1136−1143.
(42) Dutta, N. K., Alsultan, A., Gniadek, T. J., Belchis, D. A., Pinn, M. L., Mdluli, K. E., Nuermberger, E. L., Peloquin, C. A., and Karakousis, P. C. (2013) Potent rifamycin-sparing regimen cures guinea pig tuberculosis as rapidly as the standard regimen. *Antimicrob. Agents Chemother. 57*, 3910−3916.
(43) Jayaram, R., Shandil, R. K., Gaonkar, S., Kaur, P., Suresh, B. L., Mahesh, B. N., Jayashree, R., Nandi, V., Bharath, S., Kantharaj, E., and Balasubramanian, V. (2004) Isoniazid pharmacokinetics-pharmacodynamics in an aerosol infection model of tuberculosis. *Antimicrob. Agents Chemother. 48*, 2951−2957.
(44) Chan, E. D., and Iseman, M. D. (2002) Current medical treatment for tuberculosis. *BMJ 325*, 1282−1286.
(45) Rodrigues, M. O., Cantos, J. B., D'Oca, C. R., Soares, K. L., Coelho, T. S., Piovesan, L. A., Russowsky, D., da Silva, P. A., and D'Oca, M. G. (2013) Synthesis and antimycobacterial activity of isoniazid derivatives from renewable fatty acids. *Bioorg. Med. Chem. 21*, 6910−6914.
(46) Makino, K., Nakajima, T., Shikamura, M., Ito, F., Ando, S., Kochi, C., Inagawa, H., Soma, G., and Terada, H. (2004) Efficient intracellular delivery of rifampicin to alveolar macrophages using rifampicin-loaded PLGA microspheres: Effects of molecular weight and composition of PLGA on release of rifampicin. *Colloids Surf., B: Biointerfaces 36*, 35−42.
(47) Dharmadhikari, A. S., and Nardell, E. A. (2008) What animal models teach humans about tuberculosis. *Am. J. Respir. Cell Mol. Biol. 39*, 503−508.
(48) McMurray, D. N. (1994) Guinea pig model of tuberculosis. In *Tuberculosis: Pathogenesis, protection and control* (Bloom, B. R., Ed.) pp 135−147, American Society for Microbiology, Washington, DC.
(49) Ahmad, Z., Nuermberger, E. L., Tasneen, R., Pinn, M. L., Williams, K. N., Peloquin, C. A., Grosset, J. H., and Karakousis, P. C. (2010) Comparison of the 'denver regimen' against acute tuberculosis in the mouse and guinea pig. *J. Antimicrob. Chemother. 65*, 729−734.
(50) Horváti, K., Mező, G., Szabó, N., Hudecz, F., and Bősze, S. (2009) Peptide conjugates of therapeutically used antitubercular isoniazid-design, synthesis and antimycobacterial effect. *J. Pept. Sci. 15*, 385−391.
(51) Sula, L. (1963) Who co-operative studies on a simple culture technique for the isolation of mycobacteria. 1. Preparation, lyophilization and reconstitution of a simple semi-synthetic concentrated liquid medium; culture technique; growth pattern of different mycobacteria. *Bull. World Health Org. 29*, 589−606.
(52) Sula, L., and Sundaresan, T. K. (1963) Who co-operative studies on a simple culture technique for the isolation of mycobacteria. 2. Comparison of the efficacy of lyophilized liquid medium with that of loewenstein-jensen (l-j) medium. *Bull. World Health Org. 29*, 607−625.
(53) Vinsova, J., Cermakova, K., Tomeckova, A., Ceckova, M., Jampilek, J., Cermak, P., Kunes, J., Dolezal, M., and Staud, F. (2006) Synthesis and antimicrobial evaluation of new 2-substituted 5,7-di-tert-butylbenzoxazoles. *Bioorg. Med. Chem. 14*, 5850−5865.
(54) Helmerhorst, E. J., Reijnders, I. M., van 't Hof, W., Veerman, E. C., and Nieuw Amerongen, A. V. (1999) A critical comparison of the hemolytic and fungicidal activities of cationic antimicrobial peptides. *FEBS Lett. 449*, 105−110.
(55) Liu, Y., Peterson, D. A., Kimura, H., and Schubert, D. (1997) Mechanism of cellular 3-(4,5-dimethylthiazol-2-yl)-2,5-diphenyltetrazolium bromide (mtt) reduction. *J. Neurochem. 69*, 581−593.
(56) Mosmann, T. (1983) Rapid colorimetric assay for cellular growth and survival: Application to proliferation and cytotoxicity assays. *J. Immunol. Methods 65*, 55−63.
(57) Slater, T. F., Sawyer, B., and Straeuli, U. (1963) Studies on succinate-tetrazolium reductase systems. III. Points of coupling of four different tetrazolium salts. *Biochim. Biophys. Acta 77*, 383−393.
(58) Tomioka, H., Sato, K., Kajitani, H., Akaki, T., and Shishido, S. (2000) Comparative antimicrobial activities of the newly synthesized quinolone wq-3034, levofloxacin, sparfloxacin, and ciprofloxacin against mycobacterium tuberculosis and mycobacterium avium complex. *Antimicrob. Agents Chemother. 44*, 283−286.
(59) Ziegler-Heitbrock, H. W., Thiel, E., Futterer, A., Herzog, V., Wirtz, A., and Riethmuller, G. (1988) Establishment of a human cell line (mono mac 6) with characteristics of mature monocytes. *Int. J. Cancer 41*, 456−461.
(60) Horváti, K., Bacsa, B., Szabó, N., Dávid, S., Mező, G., Grolmusz, V., Vértessy, B., Hudecz, F., and Bősze, S. (2012) Enhanced cellular uptake of a new, in silico identified antitubercular candidate by peptide conjugation. *Bioconjug. Chem. 23*, 900−907.